Title
ISOMER SHIFTS OF THE 6.2-keV GAMMA RAYS OF TANTALUM-l8l

Authors
Kaindl, G.
Salomon, D.
Wortmann, G.

Publication Date
1974-09-01

LBL-3437
c.2

To be published as a Chapter in
book entitled, "Mössbauer Isomer
Shifts", G. K. Shenoy and F. E. Wagner,
eds., North-Holland Publishing Company

ISOMER SHIFTS OF THE 6.2-keV GAMMA RAYS OF TANTALUM-181

G. Kaindl, D. Salomon and G. Wortmann

September, 1974

Prepared for the U. S. Atomic Energy Commission
under Contract W-7405-ENG-48

DISCLAIMER

ISOMER SHIFTS OF THE 6.2-keV GAMMA RAYS OF TANTALUM-181

G. Kaindl[+]

Physik-Department der Technischen Universität
München, D-8046 Garching, Germany

and

Lawrence Berkeley Laboratory
University of California
Berkeley, Calif. 94720

D. Salomon and G. Wortmann
Physik-Department der Technischen Universität
München, D-8046 Garching, Germany

September 1974

1. Introduction

For the element tantalum two gamma resonances are known, which are both in monoisotopic ^{181}Ta at excitation energies of 6.2 keV and 136.2 keV. The relevant properties of these two gamma resonances, however, differ drastically. The 6.2-keV E1 transition between the $9/2^-$ [514] excited state with a lifetime of 9.8 μs and the $7/2^+$[404] groundstate of the strongly deformed ^{181}Ta nucleus has a large single-particle character. Because of its small natural width, $2\Gamma = W_o = 0.0064$ mm/s, and the favorable nuclear parameters of the levels involved, this resonance has an extremely high resolving power for the study of hyperfine interactions. On the other hand, the 136.2-keV (M1, 16% E2) transition between the $9/2^+$ first-excited rotational state, with a lifetime of 72 ps, and the $7/2^+$ groundstate is of little use in the study

+ Present address: Abteilung für Physik und Astronomie, Ruhr-Universität Bochum, D-463 Bochum, Germany.

of hyperfine interactions (STEINER et al. [1969]). Therefore, this chapter will be concerned exclusively with work on the 6.2-keV gamma resonance.

The accuracy of Mössbauer measurements of hyperfine interactions is mainly based on the relative sizes of the hyperfine interaction energy and the experimental linewidth. With conventional Mössbauer resonances, which have lifetimes of the excited nuclear states up to ~170 ns (in the case of ^{57}Fe), a rather limited resolution can only be obtained in such measurements. This is a serious drawback of Mössbauer spectroscopy, especially when compared with the methods of radiofrequency spectroscopy. It is therefore quite understandable, that considerable interest has been devoted to the few gamma resonances with lifetimes in the microsecond region, namely to those in ^{181}Ta (6.2 keV; τ = 9.8 μs), ^{67}Zn (93 keV; τ = 13.5 μs), and ^{73}Ge (13.3 keV; τ = 6.2 μs). Although, the natural widths of these three gamma resonances differ by less than a factor of two, they possess quite different properties in their resolving powers. This is because of the large differences in their gamma transition energies and in their relevant nuclear parameters.

The first successful observation of the 6.2-keV gamma resonance of ^{181}Ta was reported by STEYERT et al. [1965], but the observed resonance lines were broadened by more than a factor of 100 compared to the natural linewidth. Considerable progress was made a few years later by SAUER et al. [1968], when experimental linewidths of about 13 times the natural one were observed; this permitted the measurement of the magnetic moment of the excited nuclear state in a small external magnetic field. Despite this early success, the resonance effect could not,

however, be observed in host lattices other than tungsten and tantalum metal (SAUER [1969]).

The potential of the ^{181}Ta gamma resonance in the measurement of isomer shifts was fully realized, when SALOMON et al. [1971] were able to observe the resonance effect for ^{181}Ta impurities in many transition metals, the isomer shifts being up to about 200 times larger than the experimental linewidth. Since then isomer shifts have been reported for ^{181}Ta impurities in most of the 5d, 4d, and 3d transition metals, and in a few tantalum compounds (KAINDL et al. [1973c]). The observed isomer shifts cover a total range of ~110 mm/s; in view of the presently best experimental linewidth W = 0.069 mm/s, (WORTMANN [1971]), this represents an improvement of the resolution in Mössbauer isomer shift studies by more than one order of magnitude.

The present chapter is divided into two main parts. In the first part, the more general aspects of ^{181}Ta isomer shifts will be covered, including an estimation of $\Delta\langle r^2\rangle$ from the systematics of isomer shifts in transition metal hosts. The second part is devoted to solid-state applications, such as studies of the isomer-shift dependence on hydrostatic pressure, on temperature, and on dissolved gases, especially hydrogen.

2. Spectroscopy of the 6.2-keV Gamma Resonance.

2.1 Experimental Remarks

Isomer shifts of the 6.2-keV gamma rays of ^{181}Ta can be studied with standard Mössbauer technique in the transmission geometry. Since the ratio of lineshift to linewidth can be large, special attention must,

however, be devoted to the stability of the velocity drive. This can be met most easily by using a sinusoidal electromechanical velocity drive. An increased number of channels (~2000) should also be available in the data acquisition system. In addition, small solid angles ought to be used in order to prevent excessive geometrical broadening.

The main experimental difficulty in observing the 6.2-keV gamma resonance arises from its extreme sensitivity to impurities and lattice defects in the samples, which can give rise to an undesirable line broadening and hence loss of the Mössbauer signal. This requirement hence demands special care in the selection of suitable host lattices as well as in the preparation of sources and absorbers. Such a problem does not exist to a comparable extent for any other Mössbauer resonance.

The source preparation method presently used (SAUER [1969]; KAINDL et al. [1973c]) is based on the diffusion of ^{181}W activity into high-purity, and if available, single-crystal transition metals under ultra-high vacuum (UHV) conditions. Since the resulting linewidth is related to the impurity concentration in the sample, efforts have to be made to use ^{181}W of the highest-possible specific activity. Up to now this requirement has been incompletely met, since the activity is produced from 93% enriched ^{180}W metal in the highest available thermal neutron fluxes ($\sim 3 \cdot 10^{15}$ n/cm^{2}s) for periods up to several months. Presently, however, efforts are made to use carrier-free ^{181}W activity, which can be chemically separated from a tantalum-metal cyclotron target bombarded with deuterons (BINDER et al. [1974]). Usually, the activity is placed on the host metals in the form of an HF/HNO_3 solution: the dry residue is reduced to the metal by heating in a hydrogen atmosphere

at a temperature of ~800 °C for a period of ~1/2 hour. The diffusion of the activity is then performed at temperatures close to the melting points of the host metals, using either resistance-heating or induction-heating methods.

In many cases single-line tantalum metal absorbers have been used for analyzing the emission spectra of the various sources. Such absorbers can be easily prepared from high-purity tantalum metal foils (99.996% nominal purity) by an UHV annealing and degassing procedure, originally described by SAUER [1969]. There is strong evidence that the resulting linewidth of the absorption line can be further improved by increasing the degassing temperature (~2300 °C) and by improving the vacuum ($\sim 10^{-9}$ Torr).

Absorbers of TaC, $KTaO_3$, and $LiTaO_3$ have been prepared by sedimentation of the finely milled powders in a polystyrene-benzene solution on thin mylar foils.

2.2. Hyperfine Structure of the 6.2-keV Gamma Resonance Spectra

The nuclear parameters of the 6.2-keV gamma resonance are summarized in table 8d.1. Due to the large magnitudes of the nuclear moments of both nuclear states, widely split resonance spectra are obtained even in the presence of only small magnetic hyperfine fields or electric-field gradients. Single-line absorption spectra can therefore only be expected for cubic symmetry around the emitting and absorbing nuclei in the absence of magnetic interactions.

The best experimental linewidth so far has been obtained for a

$^{181}W(\underline{W})$ source and a tantalum metal absorber, W = 0.069 mm/s (WORTMANN [1971]), corresponding to ~11 times W_o. A typical single-line spectrum of such a source-absorber combination is shown in fig. 8d.1a. In the case of fig. 8d.1b an external magnetic field of 2.93±0.03 k0e was applied to the source, parallel to the direction of gamma ray emission, causing a magnetic splitting of the $9/2^- \rightarrow 7/2^+$ (E1) transition into 24 hyperfine components, of which only 16 (with $\Delta m = \pm 1$) are observed. Despite an appreciable linebroadening (by a factor of ~20 in this case) the hyperfine splitting is rather well resolved (KAINDL and SALOMON [1973a]).

The pronounced asymmetries of the lineshapes in both the single-line and the split spectra result from an interference between photoelectric absorption and Mössbauer absorption followed by internal conversion. This effect, which was first observed by SAUER et al. [1968], is particularly large for the 6.2-keV gamma rays due to their E1 multipolarity, the low gamma transition energy as well as the large internal conversion coefficient. This interference effect is well understood for E1 transitions (TRAMMEL and HANNON [1969]; KAGAN et al. [1969]). According to these theories the absorption spectra can be described by dispersion-modified lorentzian lines of the form

$$N(v) = N(\infty) - A\,(1 - 2\,\xi\,X) / (1 + X^2) \qquad (8\,d.1)$$

with $X = 2\,(v-v_o)/W$. Here N(v) is the intensity transmitted at relative velocity v, v_o is the position of the line, W is the full linewidth at half maximum, and A is the amplitude of the line. The parameter ξ determines the relative magnitude of the dispersion term. The experimental result for the magnitude of the dispersion term, $2\,\xi = -0.31 \pm 0.01$,

derived from single-line spectra of a tantalum metal absorber, agrees well with the theoretical prediction (KAINDL and SALOMON [1970; 1973a]). Dispersion terms of this size have to be taken into account in all 6.2-keV absorption spectra in order to deduce accurate values of the isomer shift as described in ch. 3.

An electric-quadrupole splitting of the 6.2-keV gamma rays has first been observed in a rhenium metal host (KAINDL et al. [1972a]). With a single-line Ta metal absorber the emission spectrum of a single-crystal ^{181}W(Re) source was analyzed in two directions of gamma emission, parallel and perpendicular to the [001] direction. The resulting hyperfine spectra, reproduced in fig. 8d.2 are a superposition of 11 hyperfine components, of which seven are $\Delta m = 0$ transitions, and one is a mixed transition. The solid lines in fig. 8d.2 represent the result of a simultaneous least-squares fit of both spectra with a superposition of dispersion-modified lorentzian lines. From this values for the ratio of nuclear quadrupole moments of both nuclear states, $Q(9/2) / Q(7/2) = 1.133 \pm 0.010$, for the isomer shift S, and for magnitude and sign of the nuclear quadrupole interaction in the groundstate of ^{181}Ta in rhenium metal were obtained. It is noteworthy that a fully resolved hyperfine spectrum was obtained in this case despite a rather wide experimental linewidth of about $95W_o$.

2.3 Summary of Isomer Shift Results

In addition to the discussed cases, isomer shifts have also been measured for sources of ^{181}W diffused into other transition metals, namely

Hf, Os, Ir, Pt; Nb, Mo, Ru, Rh, Pd; V, and Ni. In all of these cases a tantalum metal absorber was used to analyze the emission spectra. For the hexagonal host metals Hf, Os, and Ru electric-quadrupole split absorption spectra were observed (KAINDL and SALOMON [1972b]); in all other cases resonance spectra consisted of a single absorption line.

Single-line spectra for some of the metallic sources are shown in fig. 8d. 3. In the case of the nickel host the spectrum was recorded with the source heated above its Curie point and with the Ta absorber at room temperature (KAINDL and SALOMON [1973d]); in all other cases the measurements were performed at room temperature.

Mössbauer absorption spectra of tantalum compounds have been observed for the pentavalent alkali tantalates and for TaC (KAINDL et al. [1973c]). The results for the tantalates are presented in fig. 8d. 4 For $KTaO_3$, which has the cubic NaCl structure, a broad single line was observed, while electric-quadrupole split spectra were found for hexagonal $LiTaO_3$, and orthorhombic $NaTaO_3$. Assuming axially symmetric EFG's in these compounds, values for isomer shifts as well as for magnitudes and signs of the EFG's were obtained.

Table 8d. 2 summarizes the isomer shift results, with the usual sign convention for S: a more positive isomer shift corresponds to a higher transition energy. The largest isomer shift relative to tantalum metal so far has been observed for TaC. The observed experimental linewidths W range from $\sim 11W_o$ in the case of the tungsten source up to $\sim 800W_o$ in the case of the vanadium source. The magnitude of the observed resonance effect, varying between 20% and 0.2%, is strongly

correlated with the experimental linewidth. A graphical representation of the isomer shift results is shown in fig. 8d. 5. The total range of isomer shifts (110 mm/s) corresponds to 17,000W_o, or 1,600 times the best experimental linewidth obtained up to now. These numbers clearly demonstrate the high resolution with which solid-state effects on the electron density at the nucleus may be studied with this gamma resonance.

2. 4 Systematics of Isomer Shifts in Transition Metal Hosts

The isomer shifts of ^{181}Ta impurities in metallic hosts exhibit systematic features when plotted versus the number of electrons in the valence shells of the various host elements, as shown in fig. 8d. 6. The data arrange themselves in the form of three groups corresponding to 3d, 4d, and 5d host metals. Without exception, the transition energy decreases from a 5d to a 4d and further to a 3d host metal within the same column of the periodic table.

A similar systematic behaviour of isomer shifts has been observed with gamma resonances of ^{57}Fe(14. 4 keV) (QUAIM [1967]; WORTMANN [1973b]; WINDOW et al. [1970]; MUIR et al. [1966]), ^{99}Ru (90 keV), ^{197}Au (77 keV), and ^{193}Ir (73 keV) (KAINDL and SALOMON [1972c]; WORTMANN et al. [1973a]). Some of the details on this can be found in relevant chapters of this book. For all of these transitions the estimates for the changes of the mean-square nuclear charge radii, $\Delta \langle r^2 \rangle$, are reasonably well established (SHENOY and KALVIUS [1971]), so that information on the systematic behaviour of electron density differences at the impurity nuclei may be derived from these data. This in turn can be

used to derive an estimate for $\Delta \langle r^2 \rangle$ of the 6.2-keV gamma resonance.

The isomer shift data for impurities of ^{57}Fe, ^{99}Ru, and ^{197}Au, measured with the relevant gamma resonances, are summarized in fig. 8d.7. The respective results for ^{193}Ir impurities (WORTMANN et al. [1973a]) have been discussed in ch. 8c, and the systematic features closely resemble those observed for impurities of ^{99}Ru.

Taking into account the accepted sign of $\Delta \langle r^2 \rangle$ for these gamma resonances it is realized that $\rho(0)$ at the impurity nuclei increases from 5d via 4d to 3d homologous host metals. In the ^{181}Ta case such a behaviour of $\rho(0)$ results in a negative sign for $\Delta \langle r^2 \rangle$ from the observed isomer shift systematics. The only exceptions to this rule are found for hosts of iron and its d-electron homologues. In this column of the periodic system, however, the lattice structure changes from bcc to hcp.

Such a systematic variation of $\rho(0)$ at the impurity nuclei has been discussed theoretically be DA SILVA et al. [1971] in connection with the ^{57}Fe data, using a pseudo-potential approach. They predicted a decrease in the d-electron density at the impurity atom as the host is changed from 5d to 4d and further from 4d to 3d homologous metals. This would cause an increase in $\rho(0)$ in agreement with observation. A more quantitative description of the charge transfer in Ag-Au alloys has recently been given by GELATT and EHRENREICH [1974].

The dependence of $\rho(0)$ on the number of electrons N in the valence shells of the host elements of one transition series, is markedly different, however, for impurity atoms of ^{181}Ta as compared to those of ^{57}Fe ^{99}Ru, and ^{197}Au. This difference is quite obvious for 4d host metals: in the cases of ^{57}Fe, ^{99}Ru, and ^{197}Au, $\rho(0)$ decreases with

increasing N, while it increases for ^{181}Ta. This dependence of $\rho(0)$ on N should reflect effects of the bandstructure, the atomic volume, and the lattice type of the host metals on the electronic structure of the impurity atoms. From bandstructure effects a decrease of $\rho(0)$ with increasing N is expected, since the s character of the conduction bands of the host metals decreases in this direction. On the other hand, the atomic volumes of the host metals, derived from lattice constants, exhibit a dependence on N which might contribute to the observed increase of $\rho(0)$ with N for ^{181}Ta impurities in 3d and 4d hosts, and in 5d hosts up to rhenium. The relative strengths of the various effects, however, seem to depend strongly on the nature of the impurity atoms.

On the other hand, changes of $\rho(0)$ within a column of homologous transition metal hosts are much less affected by differences in the properties of impurity atoms than those within a transition series. In addition, the influence of the atomic volume of the host metal on $\rho(0)$ at the impurity atom is expected to be much less pronounced between homologous 4d and 5d hosts than between 3d hosts and any of the former ones. The reason for this is that the atomic volumes of homologous 4d and 5d metals are nearly equal, while those of homologous 3d metals are markedly smaller. This is demonstrated in fig. 8d. 8 where the isomer shifts of the 6.2-keV gamma rays are plotted versus those of gamma resonances of ^{57}Fe, ^{99}Ru, ^{197}Au, and ^{193}Ir for various host metals. Obviously, no overall proportionality is observed. If one compares, however, isomer shifts for pairs of homologous 5d and 4d host metals only, a close proportionality of the isomer shift differences for the various pairs is found, which expresses itself in the constant slopes of the straight solid lines in

Fig. 8d.8. Therefore, the ratios of isomer shift differences for various homologous 5d-4d host metal pairs may approximately be represented by one ratio, $\Delta S_1/\Delta S_2$, where the indices 1 and 2 refer to two gamma resonances, respectively.

2.5 Change of the Mean-Square Nuclear Charge Radius

These ratios of 5d-4d isomer-shift differences have been employed (KAINDL et al. [1973c]) to obtain an estimate for the change of the mean-square nuclear charge radius, $\Delta \langle r^2 \rangle$, using the relation

$$\frac{\Delta \langle r^2 \rangle_1}{\Delta \langle r^1 \rangle_2} = \frac{E_1 Z_2 \ \Delta S_1 \ \Delta\rho(0)_2}{E_2 Z_1 \ \Delta S_2 \ \Delta\rho(0)_1} \qquad (8d.2)$$

Here, the indices 1 and 2 refer to two separate gamma resonances with the energies E_1 and E_2 in elements with atomic numbers Z_1 and Z_2, respectively. $\Delta\rho(0)_2/\ \Delta\rho(0)_1$ stands for the ratio of the electron density difference at impurity element 2 to that at impurity element 1 for the two chemical environments in question. The main problem in this procedure consists in obtaining numbers for the ratios of $\Delta\rho(0)$ between homologous 5d and 4d host metals for the different impurity atoms. These ratios were estimated for the impurity atoms Ta, Au, Ir, Ru, and Fe from the results of free-ion SCF calculations. In the model used, the increase of $\rho(0)$ from a 5d to the homologous 4d host metal is described by an effective d→s charge transfer in the screening charge around the impurity atom, and the assumption is made that the magnitude of the effective charge transfer is approximately constant for the above impurity

atoms. This assumption seems to be approximately valid for the impurity atoms Ir, Ru, and Fe, as was concluded from a comparison of isomer shifts in 5d and 4d transition metal hosts with those of isoelectronic compounds of the elements under discussion. For Ta and Au impurities, however, the assumption is an extrapolation.

Table 8d. 4 summarizes the data that have been employed in deriving an estimate for $\Delta \langle r^2 \rangle$ of the 6.2-keV gamma transition. In column 2 the ratios of 5d-4d isomer-shift differences, $\Delta S_{Ta}/\Delta S_X$, are given for the ^{181}Ta gamma resonance relative to the four gamma resonances under discussion. The ratios of 5d-4d electron density differences, $\Delta\rho(0)_{Ta}/\Delta\rho(0)_X$, given in column 3, were obtained as described above and in more detail elsewhere (KAINDL et al. [1973c]).

With these values, the ratios of $\Delta \langle r^2 \rangle$ presented in column 4 were derived, using eq. (8d. 2). The $\Delta\langle r^2 \rangle$ values for the gamma resonances of ^{197}Au, ^{193}Ir, ^{99}Ru, and ^{57} Fe, as listed in column 5, were taken from the literature (see footnotes on Table 4). The absolute accuracy of these numbers should not be overestimated. The four estimates for $\Delta\langle r^2 \rangle$ of the 6.2-keV gamma resonance are finally given in the last column of Table 4, with a mean value of

$$\Delta\langle r^2 \rangle \simeq -5 \times 10^{-2} \text{ fm}^2.$$

This is one of the largest changes in nuclear charge radius observed until now for Mössbauer transitions (SHENOY and KALVIUS [1971]). The error bar for this $\Delta \langle r^2 \rangle$ value can only be estimated, especially since it is directly correlated with the uncertainties of the $\Delta\langle r^2 \rangle$ values from which it was derived. We think, however, that 50% is an upper

limit to this error.

3. Solid-State Applications

Up to now solid-state applications of the 6.2-keV gamma resonance have been based mainly on isomer shift measurements; this is mostly due to the attractive new opportunities which are provided by a large increase in resolving power. Using the above estimate for $\Delta\langle r^2\rangle$, a comparison with the 14.4-keV gamma resonance of ^{57}Fe can be made: it shows that comparable changes of the electronic structure of the Mössbauer atoms, like identical changes in the populations of Ta-6s or Fe-4s atomic orbitals, would cause lineshifts which are ~4000 times larger for ^{181}Ta than for ^{57}Fe, if they are measured in units of the respective natural linewidths. Taking the lineshifts in units of the respective experimental linewidths, the resolution is still by a factor of ~400 higher in the ^{181}Ta case as compared to the ^{57}Fe case.

In the following we will discuss the results of three applications, namely the influence (i) of hydrostatic pressure, (ii) of high temperatures, and (iii) of interstitially dissolved hydrogen on the isomer shifts in metallic hosts.

3.1 Pressure Shifts

The influence of pressure on the 6.2-keV gamma-resonance spectrum has been studied until now only for tantalum, tungsten, and platinum hosts (KAINDL et al. [1973e]; BINDER et al. [1974]). The

high-pressure setup developed especially for these experiments allows the application of a purely hydrostatic pressure up to about 5 kbar to the Mössbauer source. Pressures in this range are more than sufficient to shift the resonance line by more than one experimental linewidth, as can be seen from an inspection of Fig. 8d. 9. The oil-pressure cell used insures purely hydrostatic pressure, which is extremely important in avoiding further line broadenings due to the presence of uniaxial pressure or pressure gradients (SAUER [1969]). A 1. 5 mm to 2. 0 mm thick beryllium disk served as a window for the 6. 2 keV gamma rays. The details of such a pressure cell are given in ch. 6b, § 2. 2 and in fig. 6b. 4.

For the three hosts studied up to now, Ta, W, and Pt, the results can be characterized by decreasing isomer shifts with increasing pressure, and - within the limits of accuracy - by unchanged experimental linewidths. This is in agreement with the negative sign for $\Delta\langle r^2\rangle$ obtained previously, if we assume that $\rho(0)$ increases with decreasing volume. In fig. 8d. 10 the dependence of the isomer shift on pressure is shown for tungsten and tantalum hosts; the numerical results are summarized — along with those for the platinum host — in table 8d. 5.

A contribution to $(\partial S/\partial P)_T$ caused by a pressure dependence of the second-order Doppler (SOD) effect (JOSEPHSON [1960]) can be neglected in the present case due to the small gamma ray energy and the relatively large atomic mass of ^{181}Ta. Consequently, the experimental pressure shifts are interpreted as arising entirely from a pressure-induced variation of $\rho(0)$. In the last column of Table 8d. 5 derived values for the isothermal volume dependence of S_{IS} are listed, which were obtained by dividing $(\partial S/\partial P)_T$ by the respective compressibilities

given in column 3.

3.2 Temperature Shifts

Recently, a strong temperature dependence of the energy of the 6.2-keV gamma rays has been observed for several metallic hosts (KAINDL and SALOMON [1973b]; TAYLOR and STORMS [1969]). The observed temperature shifts were much larger than those expected from the SOD effect (thermal redshift) alone. Depending on the host metals, the shifts were found to vary between -32 to +8 times the thermal redshift expected for a Debye solid in the high-temperature limit; they were interpreted as arising mainly from temperature-induced changes of $\rho(0)$.

Such a dominance of the isomer shift over the SOD shift in the temperature-induced changes of the energy of Mössbauer gamma rays is unique to the ^{181}Ta gamma resonance. This is a result of both the extreme sensitivity of the energy of the 6.2-keV gamma rays to small variations of $\rho(0)$, and the large nuclear mass of ^{181}Ta as well as the low gamma ray energy, giving rise to rather small SOD shifts. In contrast to the ^{181}Ta case, temperature shifts of the ^{57}Fe and ^{119}Sn gamma resonance lines, which have been studied extensively in the past (POUND and REBKA [1960]; HOUSLEY and HESS [1967]; ROTHBERG et al. [1970]) are predominantly caused by the SOD effect. Only for $EuCu_2Si_2$ has also a strong temperature dependence of the isomer shift of the ^{151}Eu gamma resonance line been observed, which was interpreted in terms of a valency change of the Eu ion, caused by fast interconfigurational fluctuations

of electronic charge between the localized 4f level and the conduction band (BAUMINGER et al. [1973]).

The temperature shifts were measured with heated sources of ^{181}W diffused into various host metals and with a tantalum metal absorber at room temperature. The experimental results for five of the studied sources are shown in fig. 8d. 11, where the line shifts relative to a Ta metal absorber are plotted versus the temperatures of the sources. For comparison, the SOD shift expected for a Debye solid in the limit of high temperatures, is indicated by a dashed line. All curves are drawn on the same scale where solid lines represent least-squares fits of the data.

The largest variation of the line position was observed for the nickel host, where the transition energy increases with temperature with a slope which is 32 times larger and of opposite sign than the one expected from the SOD shift alone. It represents a lineshift of $\tilde{}1.1 W_o$ per degree. On the other hand, the slopes for W, Ta, and Pt hosts have the same sign as the SOD shift, but are up to eight times larger.

For the following discussion, the experimentally observed temperature variation of the line position S is written as

$$\left(\frac{\partial S}{\partial T}\right)_P = \left(\frac{\partial S_{SOD}}{\partial T}\right)_P + \left(\frac{\partial S_{IS}}{\partial T}\right)_V + \left(\frac{\partial S_{IS}}{\partial \ell nV}\right)_T \left(\frac{\partial \ell nV}{\partial T}\right)_P \qquad (3)$$

The first term accounts for the temperature variation of the SOD shift, which is given for a Debye solid in the limit of high temperatures by $-3k/2Mc$ in velocity units, amounting to $-2.30 \cdot 10^{-4}$ mm/s per degree for the present gamma transition. The second term represents the

explicit temperature dependence of the isomer shift at constant volume due to temperature-induced changes of $\rho(0)$. The third term describes the volume dependence of the isomer shift caused by thermal expansion of the lattice.

Table 8d. 6 summarizes the temperature shift data. The experimental results for $(\partial S/\partial T)_P$ are presented in column 2, while the values for the isobaric temperature dependence of the isomer shift, $(\partial S_{IS}/\partial T)_P$, which were obtained from $(\partial S/\partial T)_P$ by correcting for the SOD shift, are given in column 3. In view of the fact that these corrections are small compared to the total temperature shifts, and that the measurements were carried out in the temperature range from 300 K to about 1000 K, where the high-temperature Debye model approximately holds, this procedure is satisfactory within the desired accuracy. Also presented are representative values for the thermal expansion coefficients of the host metals (column 4), averaged over the relevant temperature region.

A separation of $(\partial S_{IS}/\partial T)_P$ into an explicitly temperature dependent part and a volume dependent part can be accomplished for tungsten, tantalum, and platinum hosts using the results of the high-pressure experiments for $(\partial S_{IS}/\partial \ln V)_T$ (see Table 8d. 5, last column). A summary of the analysis is given in table 8d. 7. Using the high-pressure results for $(\partial S_{IS}/\partial \ln V)_T$ the values for the volume-dependent part of $(\partial S_{IS}/\partial T)_P$, presented in column 2, were obtained. They have opposite signs than the total $(\partial S_{IS}/\partial T)_P$. The final results are given in column 3. In all three cases, the transition energy decreases explicityly with increasing

temperature. For the platinum host the magnitude of $(\partial S_{IS}/\partial T)_V$ is more than twice as big as for the tantalum and tungsten hosts.

Taking $\Delta \langle r^2 \rangle \simeq -5 \times 10^{-2}$ fm^2, these decreases of the transition energy correspond to increases of $\rho(0)$ by amounts of 6.4, 6.8, and 19×10^{21} cm^{-3} per degree for tantalum, tungsten, and platinum hosts, respectively. These increases in $\rho(0)$ with increasing temperature can be interpreted as arising from an effective d→s electron transfer in the conduction bands at constant volume. Using the results of relativistic Dirac-Fock calculations for free-ion configurations of tantalum (MANN [1972]), the explicit increases of $\rho(0)$ with increasing temperature are found to correspond to a transfer of approximately 10^{-5} electrons per degree to s-like conduction electron states.

Explicit temperature dependences of $\rho(0)$ have also been postulated for β-tin (ROTHBERG et al. [1970]), as well as for iron metal and dilute iron impurities in transition metal hosts (HOUSLEY and HESS [1967]; WILLIAMSON [1973]). In all of these cases, $\rho(0)$ was also found to increase explicitly with temperature by amounts corresponding to an increasing population of s-like valence band states by approximately 10^{-5} electrons per degree.

It is very unlikely that a thermal softening of the Fermi surface - as proposed by HOUSLEY and HESS [1967] - is responsible for the main part of this explicit temperature variation of $\rho(0)$. An increase in $\rho(0)$ due to thermal excitations of electrons can be expected if the s-character of valence band states is higher above E_F than below. Due to the strong depression of s-like states around E_F, typical for d-transition metal bands, the expected changes, however, are too small by one order of

magnitude to explain the observed effects.

Instead, one has to consider a mechanism affecting all conduction electrons; such is provided by the electron-phonon interaction giving rise to an effective decrease in the strength of the lattice potential as the temperature increases (KASOVSKI and FALICOV [1969]; SHRIVASTAVA [1973]). In this way the valence bands become more free-electron like, thereby increasing the s-character of the conduction electrons. KASOVSKI and FALICOV [1969] have calculated on this basis the explicit temperature dependence of the Knight shift in cadmium metal. Similarly, SHRIVASTAVA [1973] has applied this concept to a calculation of the explicit temperature dependence of the isomer shift of the 14.4-keV gamma rays of ^{57}Fe in FeF_3 (PERKINS and HAZONY [1972]). A quantitative theory of the explicit temperature variations of $\rho(0)$ for transiton metal hosts is still missing, however. Presently an extension of the high-pressure experiments to other host metals, especially to those for which temperature shifts have already been measured, is under way. With these results it will become possible to obtain further and more systematic information on the explicit variation of $\rho(0)$ as a function of temperature for the d-transition metal hosts.

3.3 Effects of Dissolved Gases

The first experiments of studying the effects of dissolved gases in metals using the 6.2-keV gamma resonance were carried out by SAUER [1969), who studied the influences of nitrogen and oxygen on the resonance line in tantalum metal. The resulting spectra were characterized by

a rapid increase of the linewidth of the resonance line with increasing impurity content, and by only modest changes of the line position.

Much more striking results have recently been obtained by HEIDEMANN et al. [1974] for hydrided tantalum metal. Isomer shift and experimental linewidth were studied at room temperature for a tantalum metal absorber as a function of the hydrogen concentration c (c is defined as the hydrogen/tantalum atom ratio). Within the studied concentration range (from c = 0 to 0.147) S was found to increase rapidly and almost linearly with c up to ~10 mm/s, while the experimental linewidth showed only a modest increase.

Previous Mössbauer investigations of metal-hydrogen systems have suffered from limited resolution as well as from the fact that the Mössbauer atoms (^{57}Fe and ^{119}Sn) were impurities in the host matrices (see for example ABLEITER and GONSER [1972]). These drawbacks could be eliminated in the work with the 6.2-keV gamma resonance.

Some typical absorption spectra of hydrided tantalum metal absorbers are presented in Fig. 8d.12. At the highest hydrogen concentration studied, c = 0.147, the resonance line is shifted to positive velocities by about 10 mm/s relative to c = 0. This is a very strong effect which can be measured with great precision. In addition it provides a means for tuning the 6.2-keV transition energy continuously over a relatively wide range.

The tantalum metal foils (~4 mg/cm^2 thick, 99.996% nominal purity) were loaded electrolytically. Prior to loading, the foils were degassed in UHV in the usual way. The maximum hydrogen concentration studied was well below the room-temperature concentration limit (c = 0.22)

for the α-phase of the Ta-H system (VÖLKL and ALEFELD [1974]). From the relative changes of the lattice constant, $\Delta a/a$, the concentrations c were determined, using a linear relationship between $\Delta a/a$ and c, $d\ell na/dc = 5.3 \cdot 10^{-2}$ (PFEIFFER [1974]). Lattice constants were measured by X-ray diffraction technique. Both the Mössbauer measurements as well as the $\Delta a/a$ measurements were performed several weeks after hydriding had taken place, when stationary conditions were reached.

In Fig. 8d. 13 the experimental results for S and W are plotted versus $\Delta a/a$ and the hydrogen concentration. The isomer shift data can be approximated by a straight line with a slope of dS/dc = +62 mm/s. Since $\Delta \langle r^2 \rangle$ is negative for the 6.2-keV gamma resonance, the observed isomer shift increases correspond to a decrease of $\rho(0)$ with increasing c.

Two main contributions are expected to contribute to the observed isomer shift variation: the first is due to a change in atomic volume and the second is caused by an explicit change of the electronic structure of tantalum due to interstitially dissolved hydrogen. The influence of lattice expansion on $\rho(0)$ is difficult to estimate in the present case. In a first approximation, it is assumed that the effect of lattice expansion on $\rho(0)$ due to dissolved hydrogen is identical to the one caused by the application of hydrostatic pressure on pure tantalum metal. Then a value of $(\partial S/\partial \ell nV)_{c=0}(d\ell nV/dc) = 22$ mm/s is obtained for the volume dependent part (where $d\ell nV/dc = 3\, d\ell na/dc = 0.159$ was used: PFEIFFER [1974]). This contribution to dS/dc which may be considered an upper limit for the volume dependent part, is represented by the dashed line in Fig. 8d. 13. Clearly, it can account for not more than about one third of the observed variation of S with c.

For the second term a lower limit of $(\partial S/\partial c)_V \geq 40$ mm/s is then obtained, corresponding to an explicit decrease of $\rho(0)$ with increasing c. This is an important physical result of this work, since it reflects the changes in the electronic structure due to interstitially dissolved hydrogen.

The models proposed for transition metal hydrides range from a pure proton model, where the electrons available from hydrogen atoms are simply thought to fill up the empty states in the valence band of the host metals in a rigid-band-like way, as far as to a model where the hydrogen is essentially anionic (LIBOWITZ [1972]). Recently, it was concluded from photoemission data on PdH (EASTMAN et al. [1971]) that a simple proton model does not sufficiently describe the electronic structure of this system. Instead, some new hydrogen-induced energy states below the bottom of the d-band of Pd were found, which were attributed to bonding electrons localized around the protons in interstitial positions.

The present isomer shift results for hydrided tantalum do not contradict a model, in which only part of the hydrogen electrons are used to fill up vacant d-band states. If we assume an electron configuration of $5d^4 6s^{\cdot 5} 6p^{\cdot 5}$ for tantalum metal (estimated from bandstructure calculations of MATTHEIS [1970]) and if we use electron densities extrapolated from Dirac-Fock calculations for a few free-ion configurations of tantalum (MANN [1972]), we find that about 50 to 100% of the hydrogen electrons have to fill up empty 5d states of tantalum, in order to account for the observed decrease of $\rho(0)$ with c. The large uncertainty is mainly connected with the uncertainty in the magnitude

of $\Delta\langle r^2\rangle$.

The observed increase of the experimental linewidth with c is plotted in the upper part (b) of Fig. 8d. 13. For the same impurity concentration it is much smaller (by a factor of about 200) than the line broadening observed for oxygen- or nitrogen-loaded tantalum absorbers (SAUER [1969]). Even for the same change in lattice constant, the hydrogen-induced line broadening is still by about one order of magnitude smaller than the one caused by oxygen or nitrogen impurities. This latter behaviour is most probably due to the extremely high jumping rates of hydrogen in metals (VÖLKL and ALEFELD [1974]). To clarify this latter point a study of the temperature dependence of the linewidth of hydrided tantalum is presently underway.

4. Prospects

It is quite obvious that the high resolving power inherent in isomer shift studies with the 6.2-keV gamma resonance opens up many other attractive possibilities in the study of solid-state effects. The low gamma ray energy, which may often produce serious experimental problems, is of definite importance in this respect, since it guarantees high recoil-free fractions even close to the melting points of practically all materials. When judging the full potentials of this gamma resonance one should keep in mind that all investigations thus far have been made with gamma resonance lines which were at least 20 times wider than W_o. There is strong indication now, however, that the experimental linewidths can be improved by using carrierfree ^{181}W activity (BINDER et al. [1974]).

References:

ABLEITER, M. and U. GONSER, 1972, in Proc. Int. Conf. on Hydrogen in Metals, p. 727 (Jülich, JÜL-CONF-6, 1972); and references therein.

BAUMINGER, E. R., D. FROINDLICH, I. NOWICK, S. OFER, I. FELNER, and I. MAYER, 1973, Phys. Rev. Letter 30, 1053.

BENNET, L. H. and J. I. BUDNIK, 1960, Phys. Rev. 120, 1812.

BINDER, J., G. KAINDL, D. SALOMON, and G. WORTMANN, 1974, Technische Universität München, unpublished results; and BINDER, J., 1974, Diplomthesis, Technische Universität München.

DA SILVA, X. A., A. A. GOMES, and J. DANON, 1971, Phys. Rev. B4, 1161.

DE WIT, S. A., G. BACKENSTOSS, C. DAUM, J. C. SENS, and H. L. ACKER, 1967, Nuclear Phys. 87, 657.

EASTMAN, D. E., J. K. CASHION, and A. C. Switendick, 1971, Phys. Rev. Letters 27, 35.

GELATT, C. G. and H. EHRENREICH, 1974, Phys. Rev. B10, 398.

HAUSER, U., 1961, Nucl. Phys. 24, 488.

HEIDEMANN, A., G. KAINDL, D. SALOMON, and G. WORTMANN, 1974, Technische Universität München, unpublished results; and HEIDEMANN, A., 1974, Diplomthesis, Technische Universität München.

HOUSLEY, R. M. and F. HESS, 1967, Phys. Rev. 164, 340; and references therein.

JOSEPHSON, B. D., 1960, Phys. Rev. Letters 4, 341.

KAGAN, Y. M., A. M. AFANASEV, and V. K. VOJTOVETSKII, 1969, Soviet Phys. JETP Letters 9, 91.

KAINDL, G. and D. SALOMON, 1970, Phys. Letters 32B, 364.

KAINDL, G., D. SALOMON, and G. WORTMANN, 1972a, Phys. Rev. Letters 28, 952.

KAINDL, G. and D. SALOMON, 1972b, Phys. Letters 40A, 179.

KAINDL, G. and D. SALOMON, 1972c, Nuclear Chemistry Division Annual Report 1972, Lawrence Berkeley Laboratory, LBL 1666, p. 213.

KAINDL, G. and D. SALOMON, 1973a, in Perspectives in Mössbauer Effect Spectroscopy, Eds. S. G. COHEN and M. PASTERNAK (Plenum Press, New York).

KAINDL, G. and D. SALOMON, 1973b, Phys. Rev. Letters 30, 579.

KAINDL, G., D. Salomon, and G. WORTMANN, 1973c, Phys. Rev. B8, 1912.

KAINDL, G. and D. Salomon, 1973d, Phys. Letters 42A, 333.

KAINDL, G., D. SALOMON, and G. WORTMANN, 1973e, Mössbauer Effect Methodology 8, 211.

KASOVSKI, R. V. and L. M. FALICOV, 1969, Phys. Rev. Letters 22, 1001.

LIBOWITZ, G. G., 1972, in Solid State Chemistry, Vol. 10, Ed. L. E. J. ROBERTS, p. 79 (Butterworth, London).

MANN, J. B., 1972, Los Alamos Scientific Laboratory, private communication.

MATTHEIS, L. F., 1970, Phys. Rev. B1, 373.

MICKLITZ, H. and P. H. BARRET, 1972, Phys. Rev. Letters 28, 1547.

MUIR Jr., A. A., K. J. ANDO, and H. M. COOGAN, 1966, Mössbauer Effect Data Index 1958-1965 (Interscience Publishers, New York).

PERKINS, H. K. and Y. HAZONY, 1972, Phys. Rev. B5, 7.

PFEIFFER, H., 1974, Technische Universität München, private communication.

POTZEL, W., F. E. WAGNER, R. L. Mössbauer, G. KAINDL, and H. E. SELTZER, 1971, Z. PHYSIK 241, 179.

POUND, R. V. and G. A. REBKA, 1960, Phys. Rev. Letters 4, 274.

QUAIM, S. M., 1967, Proc. Phys. Soc. (London) 90, 1065.

ROBERTS, L. D., D. O. PATTERSEN, J. O. THOMSON, and R. P. LEVEY, 1969, Phys. Rev. 179, 656.

ROTHBERG, G. M., S. GUIMARD, and N. BENCZER-KOLLER, 1970, Phys. Rev. B1, 136.

SALOMON, D., G. KAINDL, and D. A. SHIRLEY, 1971, Phys. Letters 36A, 457.

SAUER, C., E. MATTHIAS, and R. L. Mössbauer, 1968, Phys. Rev. Letters 21, 961.

SAUER, C., 1969, Z. PHYSIK 222, 439.

SHENOY, G. K. and G. M. KALVIUS, 1971, in Hyperfine Interactions in Excited Nuclei, Eds. G. GOLDRING and R. KALISH (Gordon and Breach, New York), p. 1201.

SHRIVASTAVA, K. N., 1973, Phys. Rev. B7, 921.

STEINER, P., E. GERDAU, W. HAUTSCH, and D. STEENKEN, 1969, Z. PHYSIK 221, 281.

STEYERT, W. A., R. D. TAYLOR, and E. K. STORMS, 1965, Phys. Rev. Letters 14, 739.

TAYLOR, R. D. and E. K. STORMS, 1969, Bull. Am. Phys. Soc. 14, 836.

TRAMMEL, G. T. and J. P. HANNON, 1969, Phys. Rev. 180, 337.

VÖLKL, J. and G. ALEFELD, 1974, in Diffusion in Solids: Recent Developments, Eds. A. S. NOWIK and J. J. BURTON (Academic Press, New York).

WINDOW, B., G. LONGWORTH, and C. E. JOHNSON, 1970, J. Phys. C 3, 2156.

WILLIAMSON, D. L., 1973, Universität des Saarlandes, Saarbrücken, Germany, preprint.

WORTMANN, G., 1971, Phys. Letters 35A, 391.

WORTMANN, G., F. E. WAGNER, and G. M. KALVIUS, 1973a, Phys. Letters 42A, 483.

WORTMANN, G., 1973b, Technische Universität München, unpublished results.

Table 8d. 1. Nuclear parameters of the 6.2-keV gamma resonance of ^{181}Ta.

		References
$7/2^+$ ground state	μ = 2.35±0.01 n.m.	(a)
	Q = 3.5±0.2 b	(b)
$9/2^-$ excited state	τ = 9.8±0.6 μs	(c)
	μ = 5.35±0.09 n.m.	(d)
	Q = 4.0±0.3 b	(e)
E1 transition	W_o = 0.0064 mm/s	
	$\Delta\langle r^2\rangle \simeq -5.10^{-2}$ fm^2	(f)
moment ratios	g(9/2)/g(7/2) = 1.77±0.02	(d)
	Q(9/2)/Q(7/2) = 1.133±0.010	(e)

a) BENNET and BUDNIK [1960]

b) DE WIT et al. [1967]

c) HAUSER [1961]

d) KAINDL and SALOMON [1973a]

e) KAINDL et al. [1972a]

f) KAINDL et al. [1973c]

Table 8d.2 Room-temperature isomer shifts of dilute impurities of ^{181}Ta in hosts of the d-transition metals and of compounds of tantalum. S = isomer shift relative to tantalum metal; W = experimental linewidth (FWHM); ϵ = magnitude of the observed resonance effect.

Source Lattice	S (mm/s)	W(FWHM) (mm/s)	ϵ (%)
V	-33.2 (5)	5.0 (10)	0.1
Ni	-39.5 (2)*	0.50 (8)	1.6
Nb	-15.26 (10)	0.19 (6)	1.5
Mo	-22.60 (10)	0.13 (4)	3.0
Ru	-27.50 (30)	1.3 (2)	0.7
Rh	-28.80 (25)	3.4 (5)	0.3
Pd	-27.80 (25)	1.3 (3)	0.3
Hf	-0.60 (30)	1.6 (4)	0.2
Ta	-0.075 (4)	0.184(6)	2.4
W	-0.860 (8)	0.069(1)	20
Re	-14.00 (10)	0.60 (4)	1.3
Os	-2.35 (4)	1.8 (2)	0.8
Ir	-1.84 (4)	1.60 (14)	0.5
Pt	+2.66 (4)	0.30 (8)	1.5
Absorber Lattice			
$LiTaO_3$	-24.04 (30)	1.6 (2)	0.9
$NaTaO_3$	-13.26 (30)	1.0 (2)	0.9
$KTaO_3$	- 8.11 (15)	1.5 (2)	0.3
TaC	+70.8 (5)	2.4 (4)	0.2

* Extrapolated to room temperature from the temperature dependence of the line position, measured above the Curie point of nickel (KAINDL and SALOMON [1973b]).

Table 8d. 3. Ratios of isomer shift differences between homologous 4d and 5d transition metal hosts for the ^{181}Ta gamma resonance to those of gamma resonances of ^{197}Au (77keV), ^{193}Ir (73 keV), ^{99}Ru(90 keV), and ^{57}Fe (14. 4 keV).

X	$\Delta S(^{181}Ta)/\Delta S(X)$				
	Nb-Ta	Mo-W	Ru-Os	Rh-Ir	Pd-Pt
^{197}Au	- 54 (6)	-29 (2)	- 28 (2)	-27 (2)	-29 (2)
^{193}Ir	- 57 (10)	-59 (14)	- 58 (3)	-44 (2)	-47 (3)
^{99}Ru	-276 (57)	-235 (27)	-231 (14)	-223 (19)	-248 (31)
^{57}Fe	253 (84)	240 (27)	419 (140)	245 (22)	179 (10)

Table 8d. 4 Derivation of $\Delta\langle r^2\rangle$ of the 6.2-keV gamma resonance from systematics of isomer shifts in transition metal hosts.

Gamma Resonance	$\frac{\Delta S_{Ta}}{\Delta S_x}$	$\frac{\Delta\rho(0)_{Ta}}{\Delta\rho(0)_x}$	$\frac{\Delta\langle r^2\rangle_{Ta}}{\Delta\langle r^2\rangle_X}$	$\Delta\langle r^2\rangle_X$ (10^{-3} fm^2)	$\Delta\langle r^2\rangle_{Ta}$ (10^{-3} fm^2)
^{197}Au, 77 keV	-30	0.50	-5.2	9[a]	-47
^{193}Ir, 73 keV	-49	0.69	-6.4	4.6[b]	-29
^{99}Ru, 90 keV	-236	5.9	-1.7	25[c]	-43
^{57}Fe, 14.4 keV	218	11.5	2.9	-25[d]	-72
				Average	-48

(a) ROBERTS et al. [1969]
(b) SHENOY and KALVIUS [1971]
(c) POTZEL et al. [1971]
(d) MIKLITZ and BARRET [1972]

Table 8d. 5. Summary of pressure-shift results for tantalum, tungsten, and platinum metal hosts.

host metal	$(\partial S/\partial P)_T$ (10^{-2} mm/s/kbar)	$(\partial \ell nV/\partial P)_T$ (10^{-4} kbar^{-1})	$(\partial S_{IS}/\partial \ell nV)_T$ (mm/s)
Ta	-7.2 (6)	-5.10	140 (15)
W	-6.9 (5)	-3.16	220 (20)
Pt	-7.8 (15)	-3.5	223 (42)

Table 8d.6. Summary of temperature shifts for dilute impurities of ^{181}Ta in transition metal hosts.

host metal	$(\partial S/\partial T)_P$ (10^{-4} mm/s/deg.)	$(\partial S_{IS}/\partial T)_P$ (10^{-4} mm/s/deg.)	$(\partial \ell nV/\partial T)_P$ (10^{-5} deg.$^{-1}$)
Ni	73.2 (35)	75.5 (35)	5.2
Nb	9.2 (10)	11.5 (10)	2.5
Mo	3.6 (6)	5.9 (5)	1.7
Pd	-16.7 (70)	-14.4 (70)	3.5
Ta	-8.0 (5)	-5.7 (5)	2.0
W	-7.1 (2)	-4.8 (2)	1.4
Ir	-10.7 (33)	-8.4 (33)	2.0
Pt	-17.6 (9)	-15.3 (9)	2.9

Table 8d.7. Analysis of temperature shifts for tantalum, tungsten, and platinum hosts.

host metal	$(\partial S_{IS}/\partial \ell nV)_T(\partial \ell nV/\partial T)_P$ (10^{-4} mm/s/deg.)	$(\partial S_{IS}/\partial T)_V$ (10^{-4} mm/s/deg.)
Ta	28 (3)	-34 (4)
W	31 (3)	-36 (4)
Pt	65 (12)	-80 (13)

Figure Captions:

Fig. 8d. 1. Absorption spectra of the 6. 2-keV gamma rays, recorded with a ^{181}W(W) source and a single-line tantalum metal absorber: (a) unsplit source, (b) source in a longitudinal magnetic field of 2. 93±0. 03 kOe.

Fig. 8d. 2. Hyperfine structure of the 6. 2-keV gamma rays in rhenium metal at room temperature, with direction of gamma emission parallel (c) and perpendicular (b) to the [001] direction, respectively. In (a) the positions and intensities of the individual components are represented by solid lines ($\Delta m=\pm 1$) and dashed lines ($\Delta m=0$, case b), respectively.

Fig. 8d. 3. Single-line absorption spectra for sources of ^{181}W diffused into various transition metals.

Fig. 8d. 4. Mössbauer absorption spectra of alkali tantalates at room temperature, recorded with a ^{181}W(W) source. The centers of the electric-quadrupole split spectra are indicated by arrows.

Fig. 8d. 5. Graphical representation of isomer shifts of the 6. 2-keV gamma rays for tantalum compounds and for dilute impurities of ^{181}Ta in transition metal hosts.

Fig. 8d. 6. Systematics of isomer shifts of the 6. 2-keV gamma rays for dilute impurities of ^{181}Ta in transition metal hosts.

Fig. 8d. 7. Systematics of isomer shifts for dilute impurities of ^{57}Fe, ^{99}Ru, an d ^{197}Au, measured with gamma resonances of the impurity atoms at 14. 4 keV, 90 keV, and 77 keV, respectively.

Fig. 8d. 8. Isomer shifts of the 6. 2-keV gamma resonance versus those of gamma resonances of ^{57}Fe (14. 4 keV), ^{99}Ru (90 keV), and ^{197}Au(77 keV),

for various host metals.

Fig. 8d. 9. Emission spectra of a ^{181}W(W)source at atmospheric pressure and at 3 kbar, analyzed with a tantalum metal absorber.

Fig. 8d. 10. Variation of isomer shift as a function of applied pressure for a ^{181}W(W) source (main figure) and for a ^{181}W(Ta) source (insert).

Fig. 8d. 11. Temperature variations of the positions of absorption lines for heated sources of ^{181}W in nickel, niobium, tungsten, tantalum, and platinum host metals.

Fig. 8d. 12. Room-temperature absorption spectra for a tantalum metal absorber with various concentrations of interstitially dissolved hydrogen. The spectra were recorded with a ^{181}W(W) source.

Fig. 8d. 13. Isomer shift (a) and experimental linewidth (b) for a hydrided tantalum metal absorber as a function of $\Delta a/a$. The dashed line represents an upper limit for the contribution due to lattice expansion (see text).

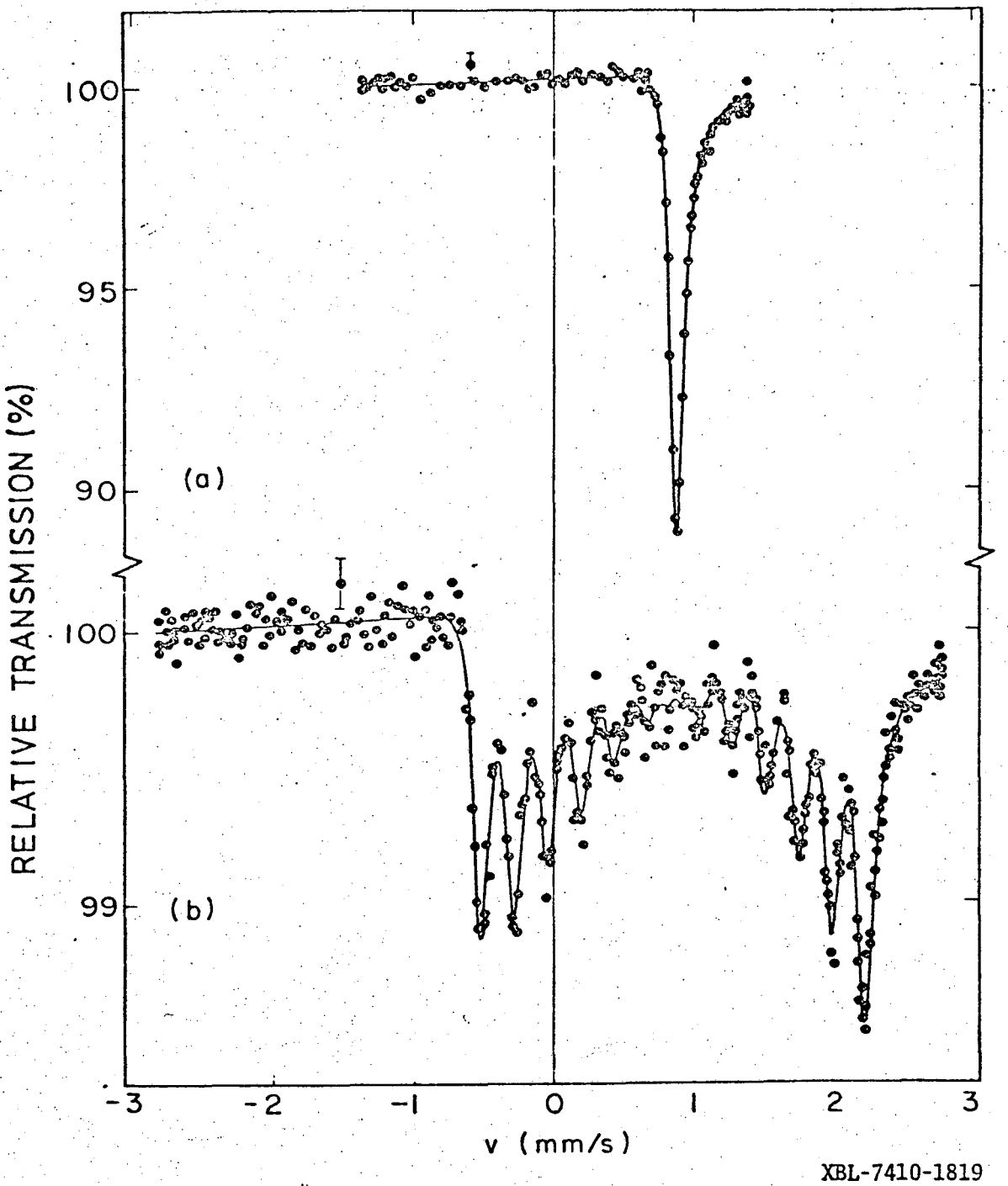
100
95
90
100
99
(a)
(b)
RELATIVE TRANSMISSION (%)
-3
-2
-1
0
1
2
3
v (mm/s)
XBL-7410-1819

Fig. 8d.1

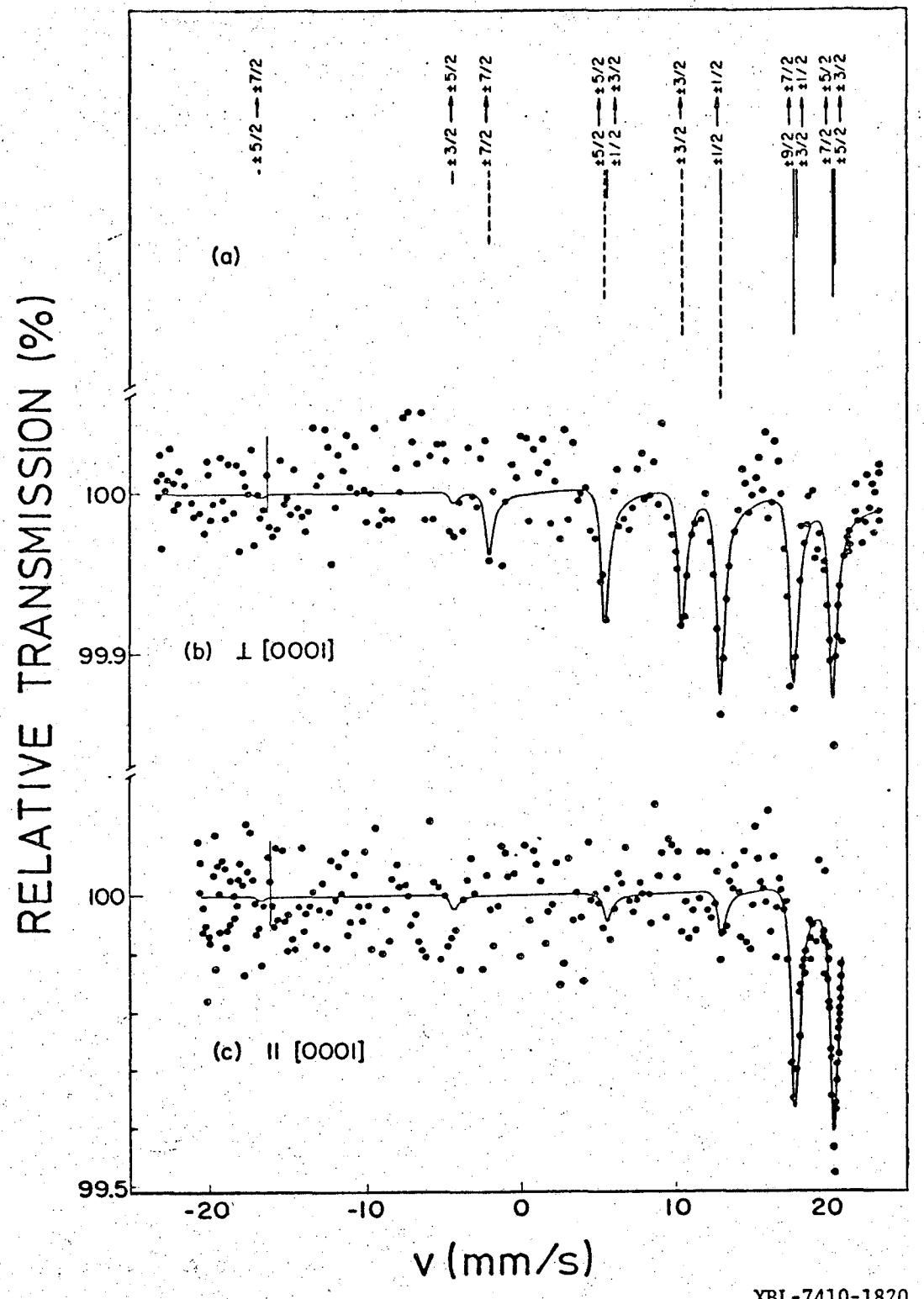
±5/2 — ±7/2
±3/2 — ±5/2
±7/2 — ±7/2
±5/2 — ±5/2
±1/2 — ±3/2
±3/2 — ±3/2
±1/2 — ±1/2
±9/2 — ±7/2
±3/2 — ±1/2
±7/2 — ±5/2
±5/2 — ±3/2
(a)
100
99.9
(b) ⊥ [0001]
100
99.5
(c) ∥ [0001]
RELATIVE TRANSMISSION (%)
-20
-10
0
10
20
v (mm/s)
XBL-7410-1820

Fig. 8d.2

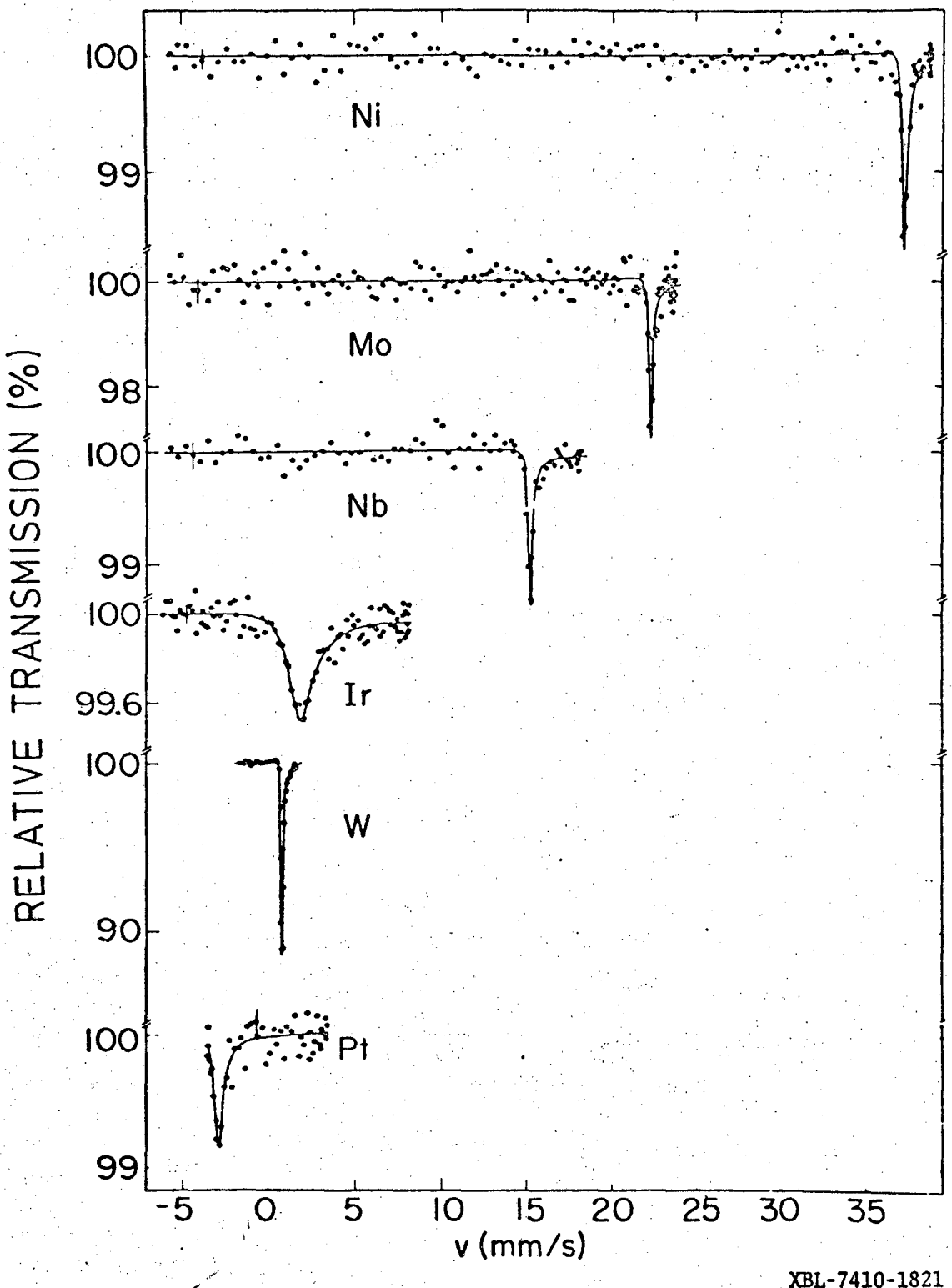
RELATIVE TRANSMISSION (%)
100
99
Ni
100
98
Mo
100
99
Nb
100
99.6
Ir
100
90
W
100
99
Pt
-5
0
5
10
15
20
25
30
35
v (mm/s)
XBL-7410-1821

Fig. 8d.3

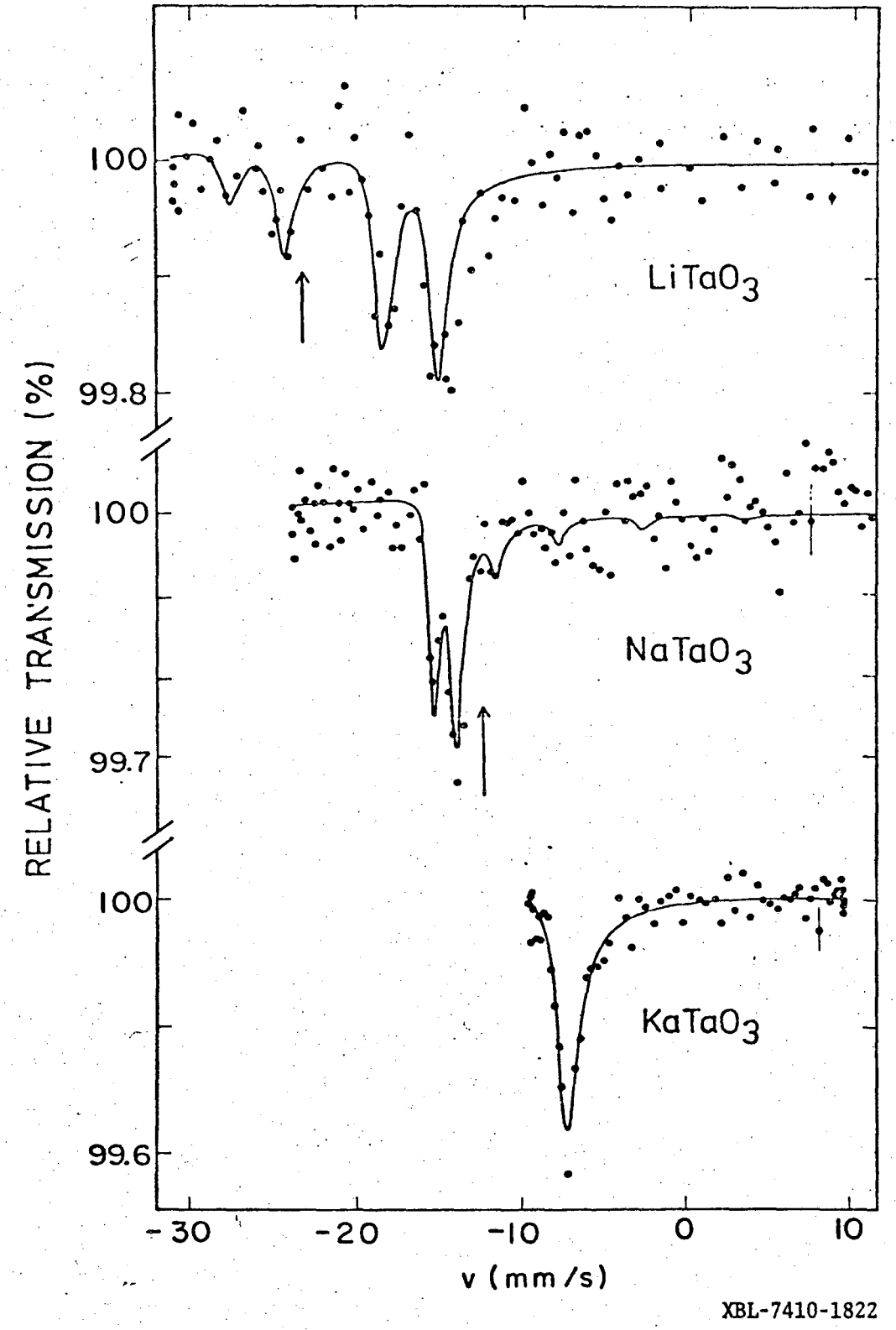
RELATIVE TRANSMISSION (%)
100
99.8
LiTaO3
100
99.7
NaTaO3
100
99.6
KaTaO3
-30
-20
-10
0
10
v (mm/s)
XBL-7410-1822

Fig. 8d.4

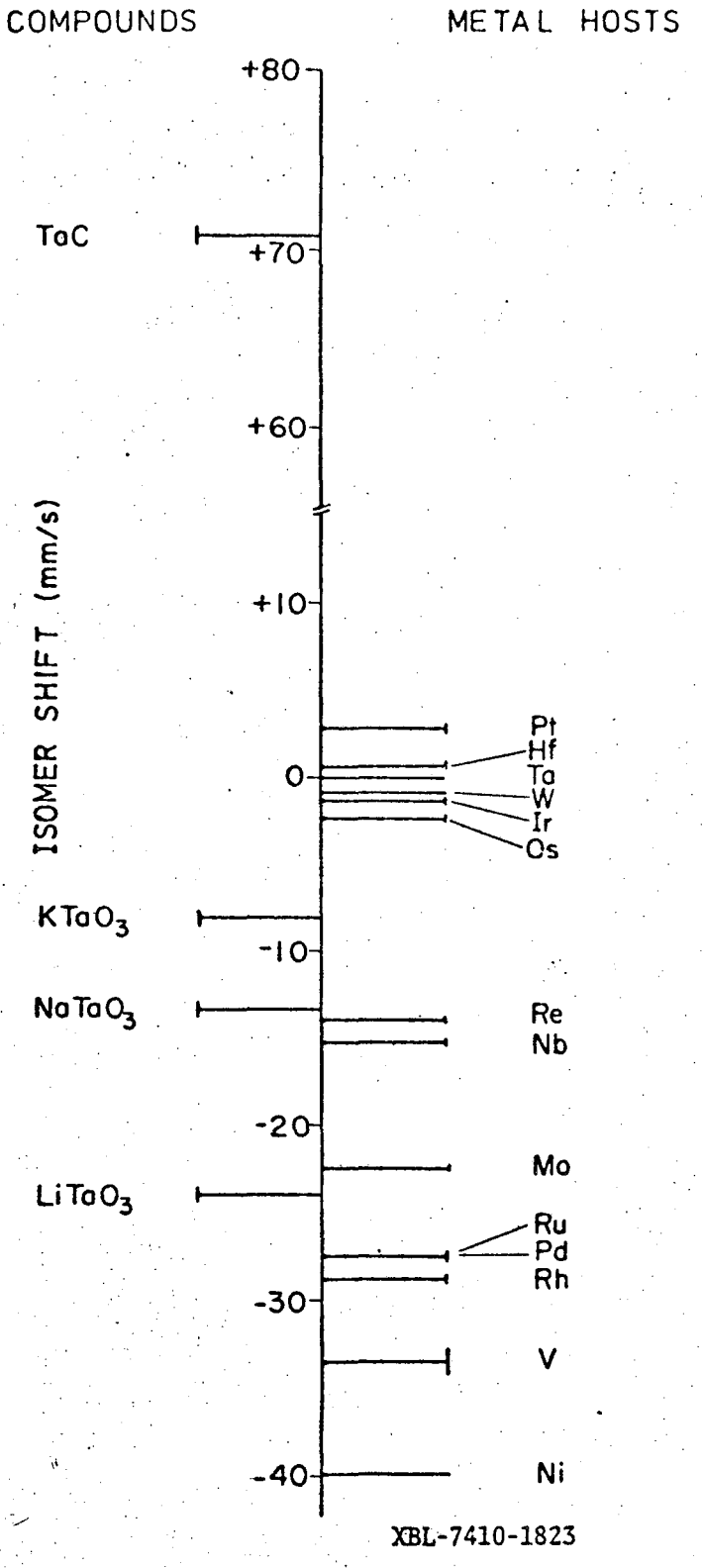
COMPOUNDS
METAL HOSTS
+80
+70
+60
+10
0
-10
-20
-30
-40
ISOMER SHIFT (mm/s)
TaC
KTaO3
NaTaO3
LiTaO3
Pt
Hf
Ta
W
Ir
Os
Re
Nb
Mo
Ru
Pd
Rh
V
Ni
XBL-7410-1823

Fig. 8d.5

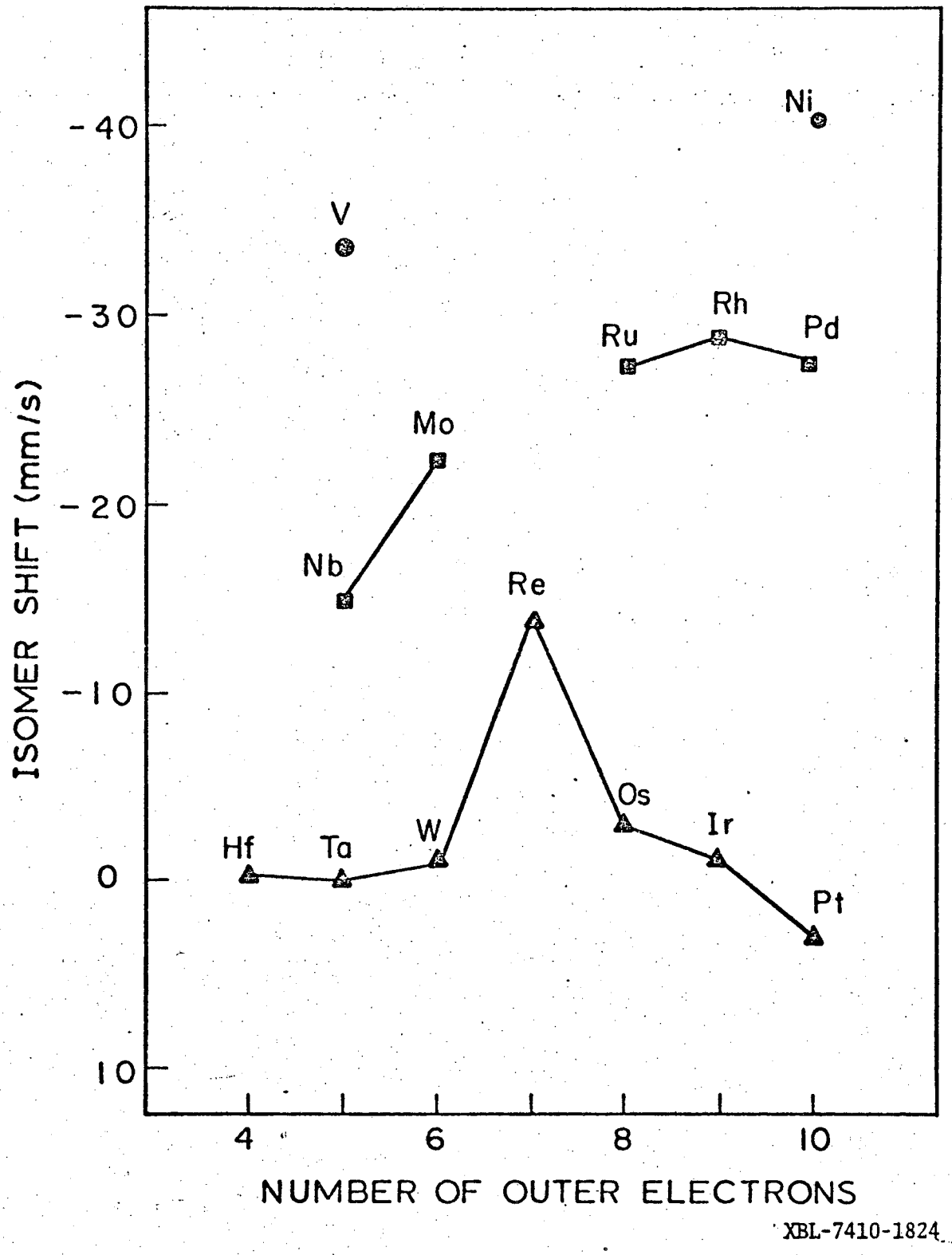
-40
-30
-20
-10
0
10
ISOMER SHIFT (mm/s)
Ni
V
Rh
Ru
Pd
Mo
Nb
Re
Os
Ir
W
Hf
Ta
Pt
4
6
8
10
NUMBER OF OUTER ELECTRONS
XBL-7410-1824

Fig. 8d.6

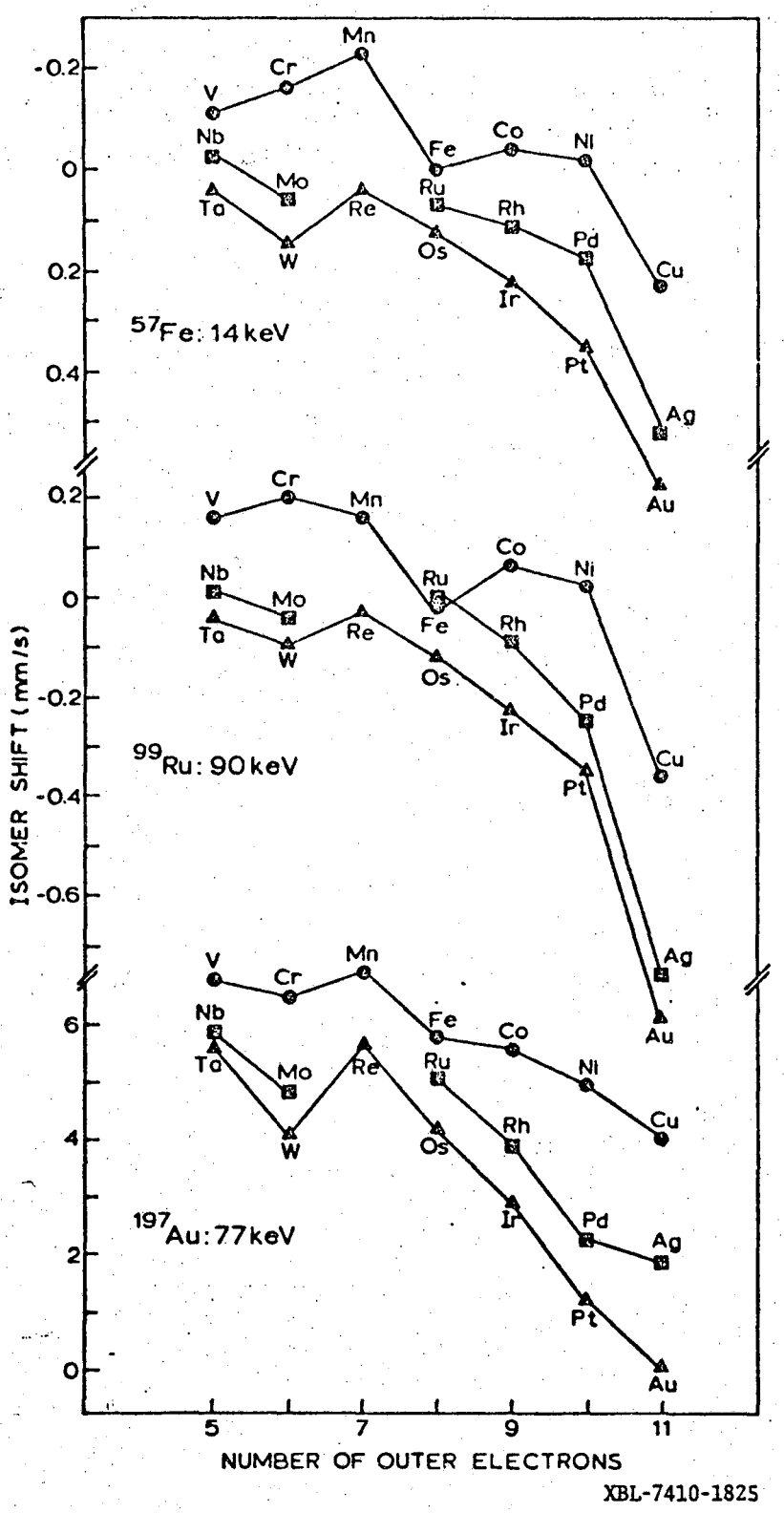
ISOMER SHIFT (mm/s)
NUMBER OF OUTER ELECTRONS
^{57}Fe: 14 keV
^{99}Ru: 90 keV
^{197}Au: 77 keV
V
Cr
Mn
Fe
Co
Ni
Cu
Nb
Mo
Ru
Rh
Pd
Ag
Ta
W
Re
Os
Ir
Pt
Au
XBL-7410-1825

Fig. 8d. 7

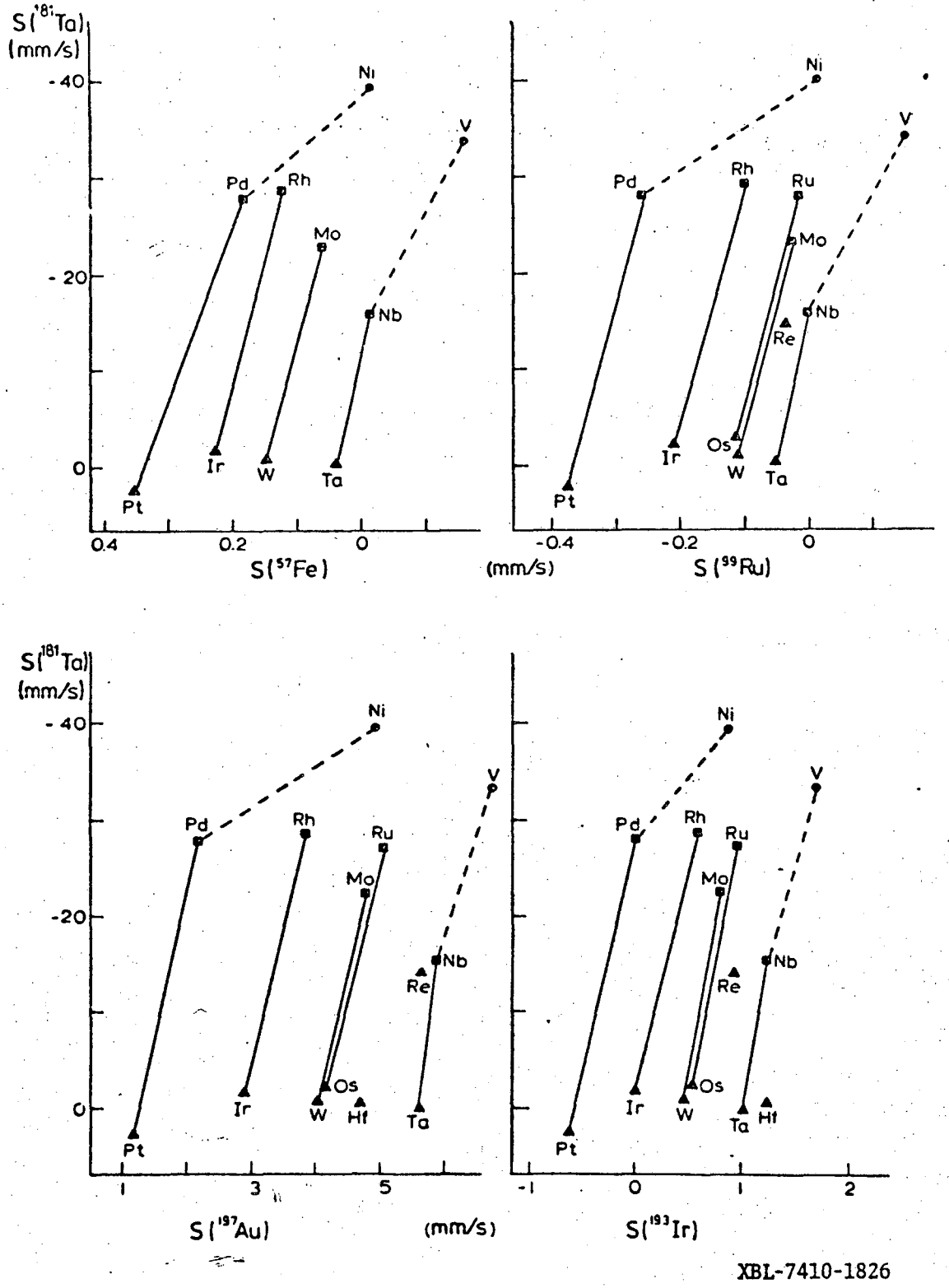
S(181Ta) (mm/s)
-40
-20
0
Ni
V
Pd
Rh
Mo
Nb
Ir
W
Ta
Pt
0.4
0.2
0
S(57Fe)
Ni
V
Pd
Rh
Ru
Mo
Nb
Re
Ir
Os
W
Ta
Pt
-0.4
-0.2
0
(mm/s)
S(99Ru)
S(181Ta) (mm/s)
-40
-20
0
Ni
V
Pd
Rh
Ru
Mo
Nb
Re
Os
Ir
W
Hf
Ta
Pt
1
3
5
S(197Au)
(mm/s)
-1
0
1
2
S(193Ir)
XBL-7410-1826

Fig. 8d.8

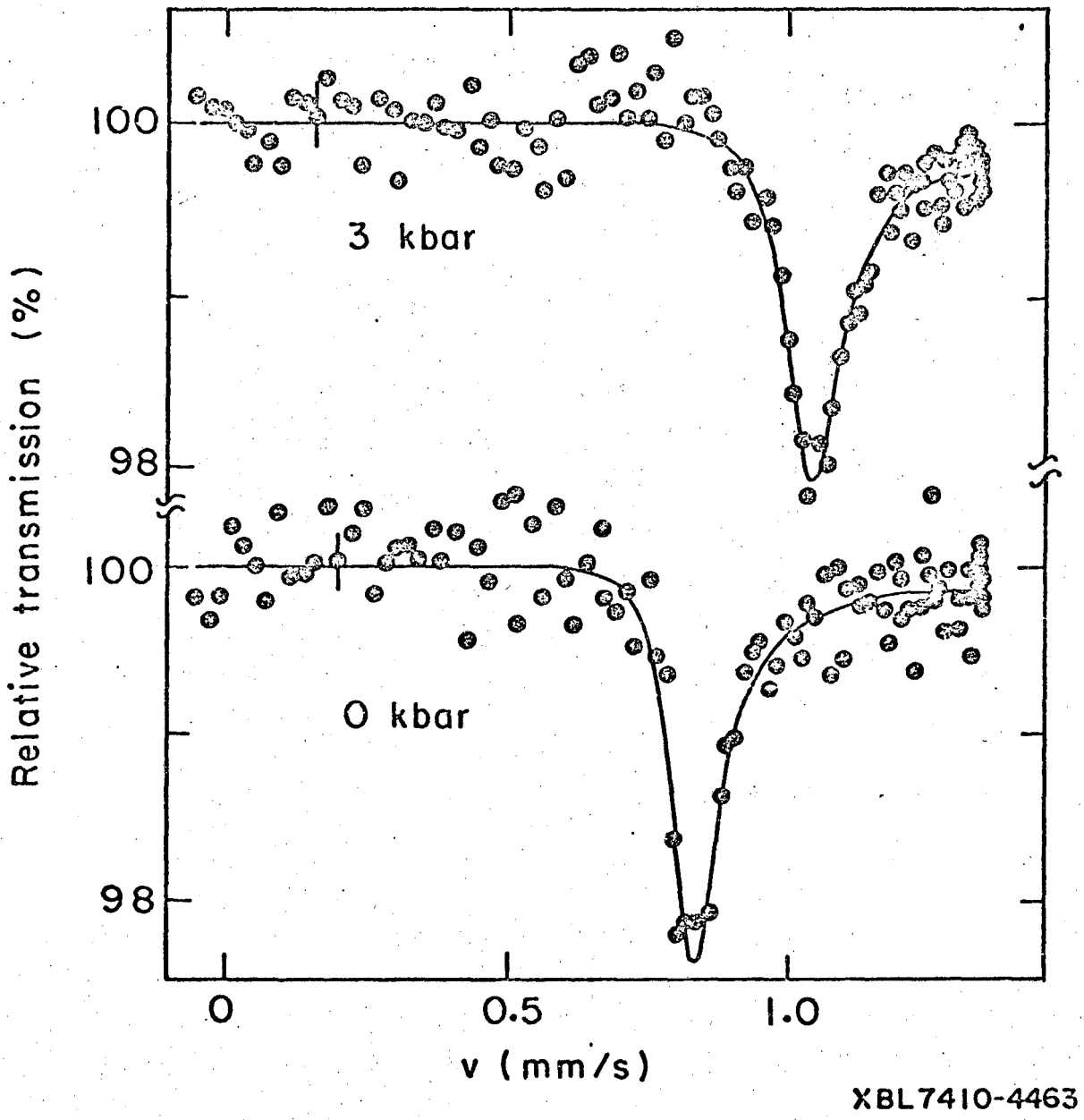
100
3 kbar
98
100
0 kbar
98
Relative transmission (%)
0
0.5
1.0
v (mm/s)
XBL7410-4463

Fig. 8d.9

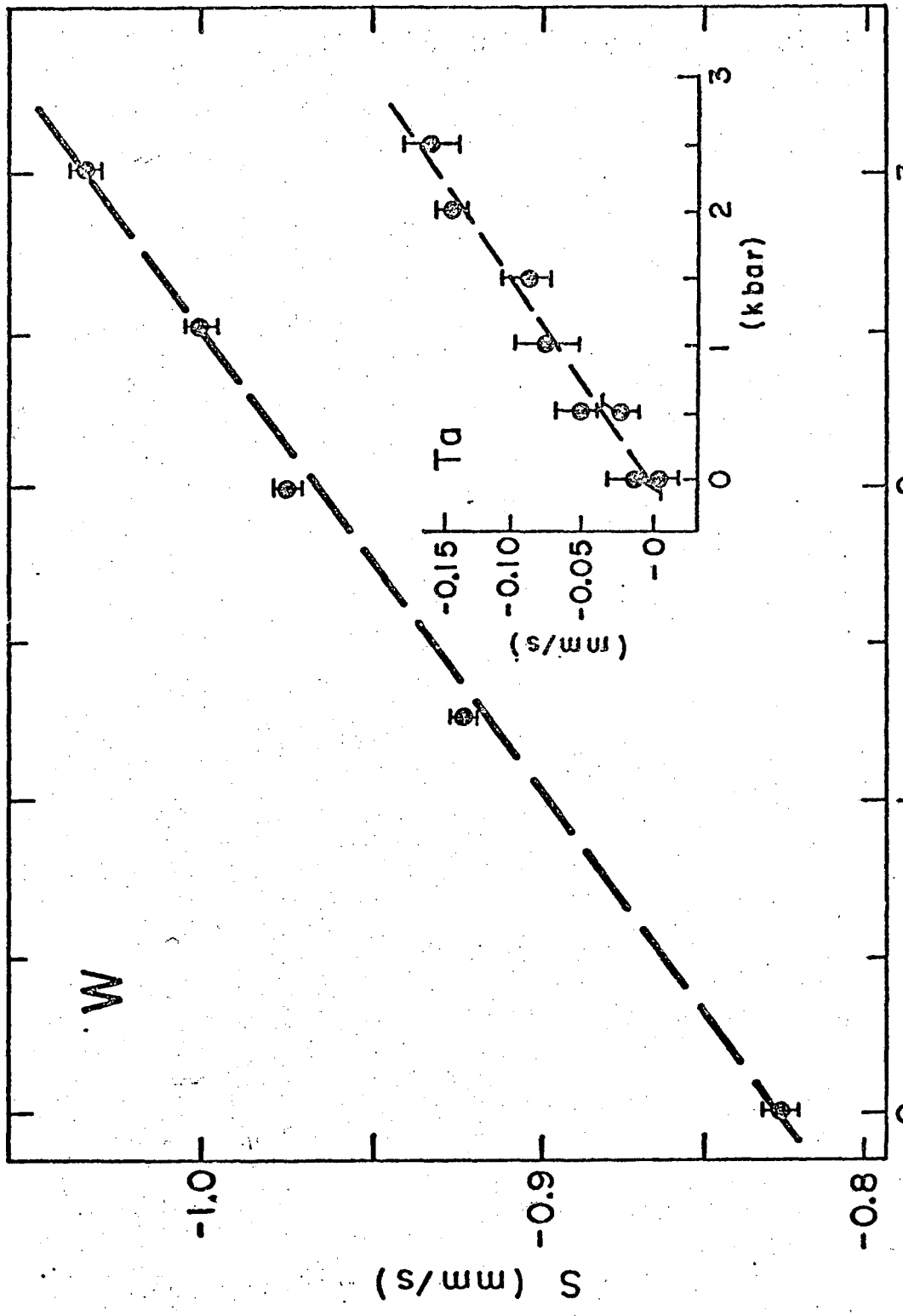
W
Ta
S (mm/s)
-1.0
-0.9
-0.8
0
1
2
3
Pressure P (kbar)
-0.15
-0.10
-0.05
-0
(mm/s)
0
1
2
3
(kbar)
XBL7410-4462

Fig. 8d.10

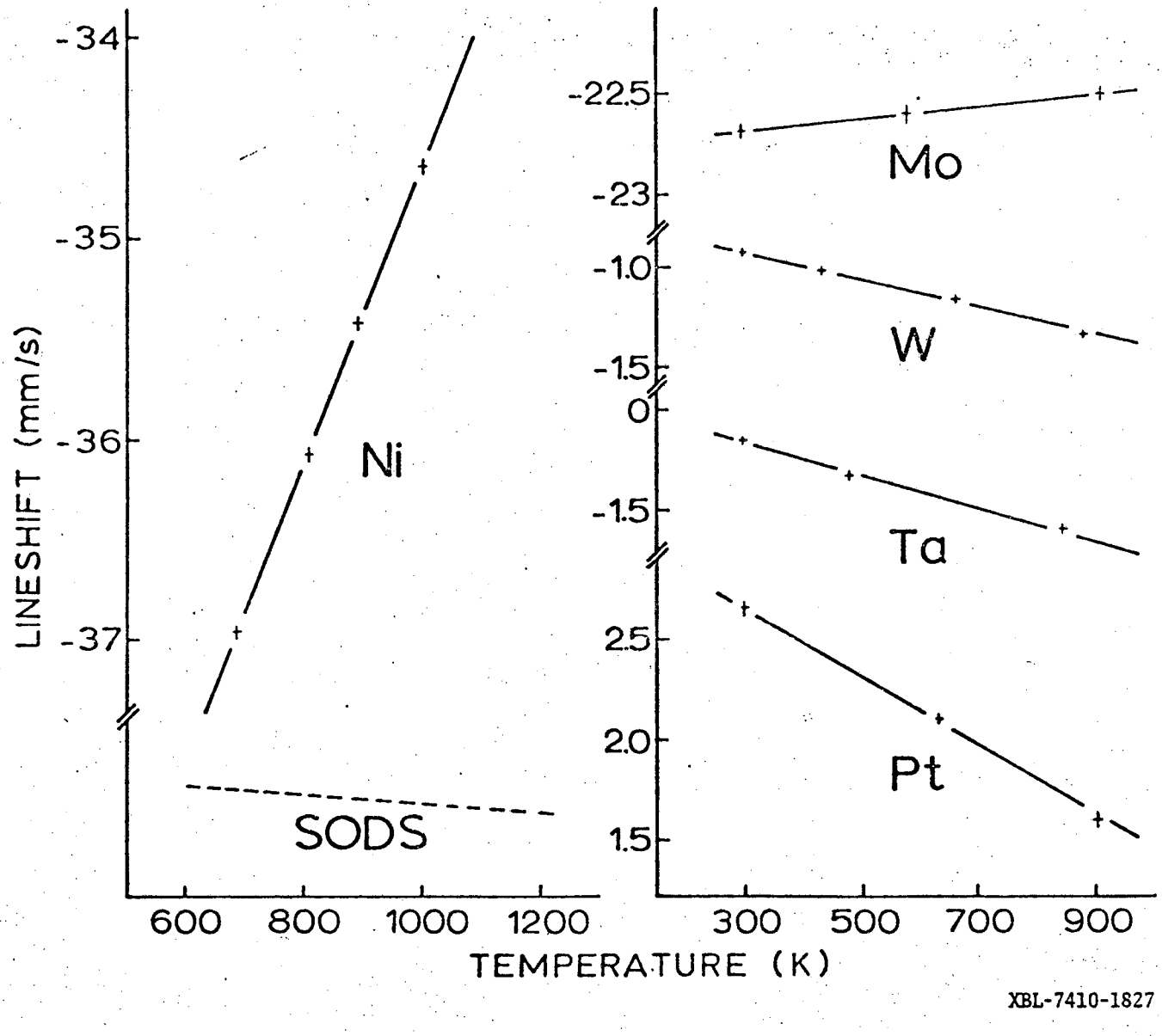
-34
-35
-36
-37
LINESHIFT (mm/s)
Ni
SODS
600
800
1000
1200
-22.5
-23
-1.0
-1.5
0
-1.5
2.5
2.0
1.5
Mo
W
Ta
Pt
300
500
700
900
TEMPERATURE (K)
XBL-7410-1827

Fig. 8d.11

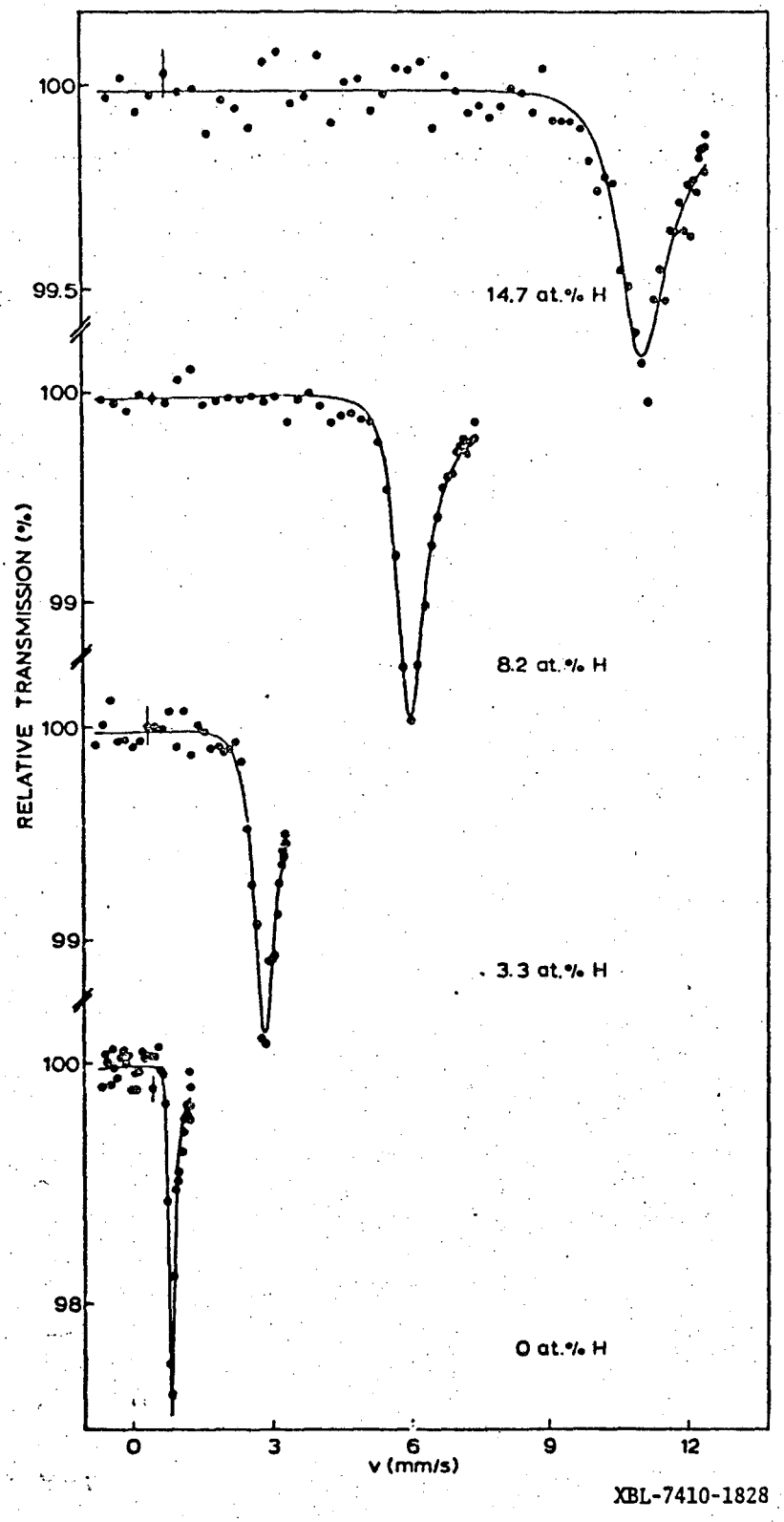
100
99.5
14.7 at.% H
100
99
8.2 at.% H
100
99
3.3 at.% H
100
98
0 at.% H
RELATIVE TRANSMISSION (%)
0
3
6
9
12
v (mm/s)
XBL-7410-1828

Fig. 8d.12

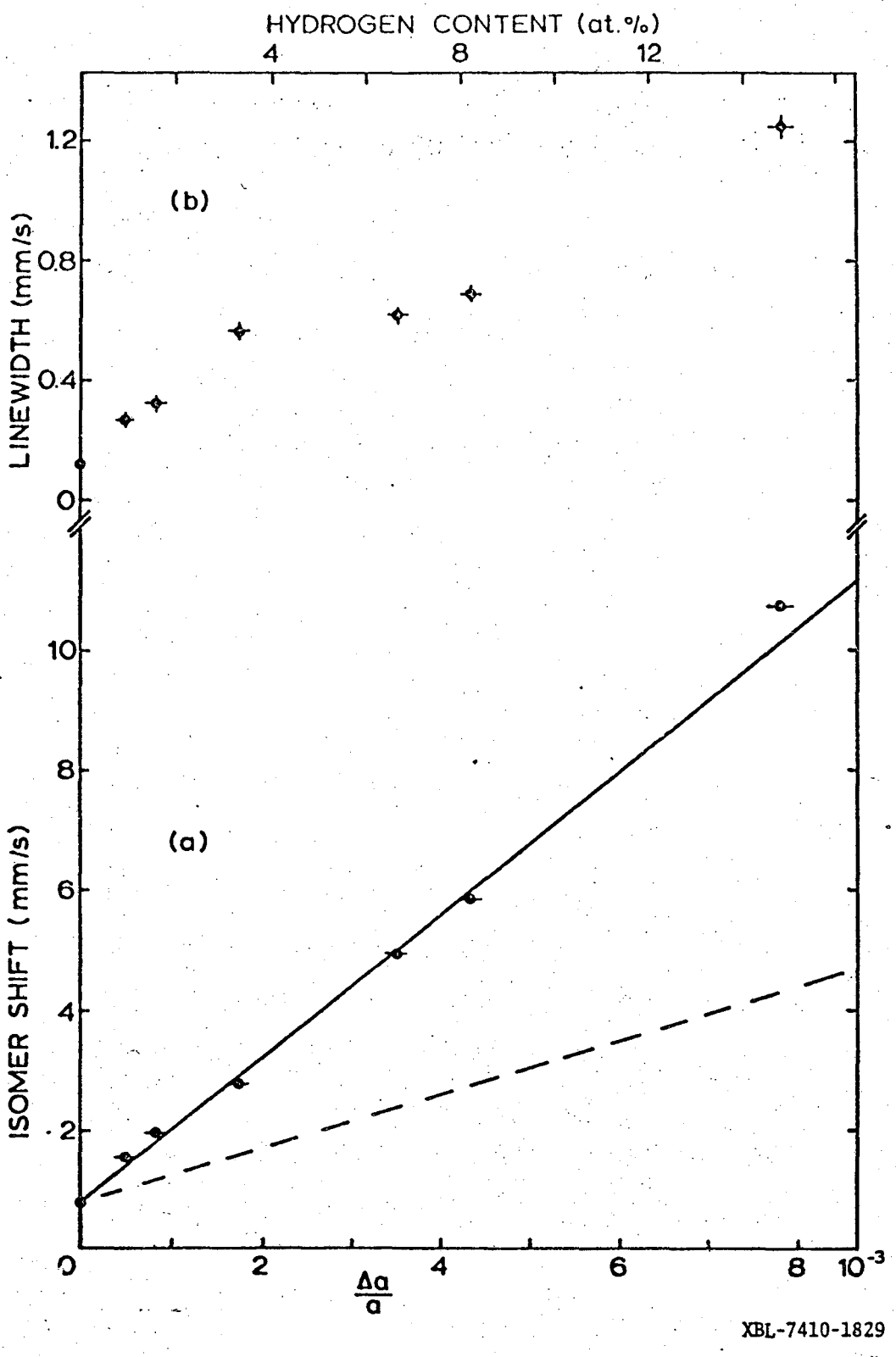
HYDROGEN CONTENT (at.%)
4
8
12
1.2
0.8
0.4
0
LINEWIDTH (mm/s)
(b)
10
8
6
4
2
0
ISOMER SHIFT (mm/s)
(a)
2
4
6
8
10-3
Δa/a
XBL-7410-1829

Fig. 8d.13

TECHNICAL INFORMATION DIVISION
LAWRENCE BERKELEY LABORATORY
UNIVERSITY OF CALIFORNIA
BERKELEY, CALIFORNIA 94720